

Superexchange interaction in cuprates

Y. Mizuno,* T. Tohyama, and S. Maekawa

Institute for Materials Research, Tohoku University, Sendai 980-8577, Japan

(Received 20 August 1998)

Recent experiments have shown that the superexchange interaction J in one-dimensional (1D) cuprates is larger than that in two-dimensional (2D) ones. We investigate a microscopic origin of the difference of J in the 1D and 2D cuprates. The hopping matrix elements between $\text{Cu}3d$ and $\text{O}2p$ orbitals and between $\text{O}2p$ orbitals are considerably influenced by the Madelung potential, which is a function of crystal structure, and these values in the 1D cuprates are enhanced as compared with those for the 2D ones, resulting in larger values of J . The same mechanism is applied to hopping matrix elements in the ladder cuprates. The elements between $\text{O}2p$ orbitals are found to be responsible for the anisotropic J 's along leg and rung of the ladder; i.e., $J_{\text{leg}} > J_{\text{rung}}$. We find a unique dependence of the electronic structure of cuprates on the dimensionality. [S0163-1829(98)52546-5]

Superexchange interaction J in insulating cuprates contains much information on the electronic states of the materials. Recent magnetic measurements on insulating cuprates demonstrate remarkable dependence of the interaction on the dimensionality of Cu-O network.¹⁻⁹ This provides us a good opportunity to establish proper understanding of the electronic states of the cuprates.

Since the discovery of high- T_c superconductivity, J in two-dimensional (2D) cuprates has been extensively studied by using several experimental tools, and is now known to be not strongly dependent on materials with the magnitude of 0.1 eV~0.16 eV.¹⁻³ On the contrary, the value of J in one-dimensional (1D) corner-sharing Cu-O chains has been reported to be 0.17 eV~0.23 eV from susceptibility measurements^{4,5} and 0.23 eV~0.26 eV from optical absorption measurements.⁶ These numbers are apparently larger than those in the 2D cuprates. This indicates the difference of the electronic states between the 1D and 2D cuprates. More interestingly, the value of J in two-leg ladder compounds shows large anisotropy: the exchange coupling along leg (rung) of the ladders J_{leg} (J_{rung}) is 0.17 (0.09) eV in SrCu_2O_3 (Ref. 7), 0.13 (0.072) eV (Ref. 8), and 0.16 (0.08) eV (Ref. 9) in $\text{Sr}_{14}\text{Cu}_{24}\text{O}_{41}$.

In this paper, we report a possible microscopic origin of the variation of J in the cuprates. Examining the Madelung potentials around Cu and O ions, we find that hopping matrix elements between $\text{Cu}3d$ and $\text{O}2p$ orbitals, t_{pd} , and between $\text{O}2p$ orbitals, t_{pp} , are significantly influenced by the potentials. In the 1D cuprates, these magnitudes are enhanced as compared with that in 2D, resulting in large J which is consistent with the experimental results. In the ladder compounds containing a coupled two-leg ladder structure, hopping matrix elements between $\text{O}2p$ orbitals along the leg of the ladder are enhanced by the presence of adjacent two-leg ladders. This makes J along the leg larger than that along the rung. Thus, we find a unique dependence of the electronic structure of cuprates on the dimensionality.

Figure 1 shows the underlying structure of Cu-O network. For the 1D cuprates, there are two types of structure: a simple corner-sharing Cu-O chain seen in Sr_2CuO_3 and Ca_2CuO_3 [Fig. 1(a)] and a double chain seen in SrCuO_2 [Fig.

1(b)].¹⁰ In Fig. 1(b), two chains are combined by the edge-sharing structure, where the bond angle of Cu-O-Cu is near 90 degrees. The two-leg ladder structure is shown in Fig. 1(c). Such isolated ladders are seen in $\text{LaCuO}_{2.5}$.¹¹ Other ladder compounds such as SrCu_2O_3 (Ref. 12) and $(\text{Sr, Ca})_{14}\text{Cu}_{24}\text{O}_{41}$ (Ref. 13) have the coupled two-leg ladder structure, where two ladders are combined by the edge-sharing structure as for the double chains in Fig. 1(b). The 2D corner-sharing CuO_2 plane [Fig. 1(d)] is seen in the high- T_c cuprates.

In the perturbation theory for cuprates, J is expressed by an equation¹⁴ containing hopping energies, t_{pd} and t_{pp} , energy-level separation between $\text{Cu}3d$ and $\text{O}2p$ orbitals, Δ , and on-site Coulomb energies on $\text{Cu}3d$ and $\text{O}2p$, U_d and U_p . The hopping energies appear in numerator of the ex-

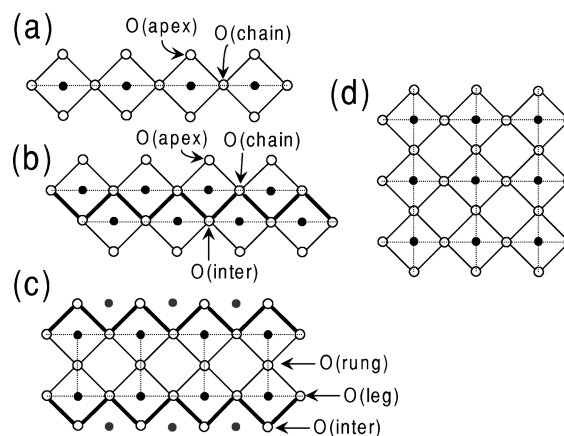


FIG. 1. Various types of network made by Cu and O atoms. (a) 1D corner-sharing CuO_3 chain, (b) double chain, (c) Cu_2O_5 two-leg ladder, and (d) 2D CuO_2 plane. Solid and open symbols denote Cu and O atoms, respectively. O(chain) and O(apex) denote the oxygens combining with Cu atoms in the parallel and perpendicular directions to the chain, respectively. In the ladder cuprates (c), three spatially nonequivalent oxygens are denoted by O(leg), O(rung), and O(inter). The hatched circles represent Cu ions in adjacent ladders of a coupled ladder structure. There are two kinds of the O-O bond in (b) and (c) that are denoted by the thin and bold lines.

pression, while the others in its denominator. Therefore, the increase in t_{pd} and t_{pp} (Δ and the Coulomb energies) leads to the enhancement (reduction) of J . Since the Coulomb energies are supposed to be independent of material, the variation of J should come from the hopping matrix elements (t_{pd} and t_{pp}) and/or Δ . The charge-transfer gap experimentally observed in the 1D cuprates is generally larger than that in 2D,¹⁵ implying larger Δ for 1D.¹⁶ This indicates that Δ is never the origin of the variation of J , but t_{pd} and t_{pp} should be. Hereafter, we regard t_{pd} and t_{pp} as hopping matrix elements for a hole.

By using a $\text{Cu}3d$ Wannier orbital, ϕ_d , at \mathbf{r}_{Cu} and an adjacent $\text{O}2p$ Wannier orbital, ϕ_p , at \mathbf{r}_{O} , t_{pd} is defined as

$$t_{pd} = \int \phi_p^*(\mathbf{r}-\mathbf{r}_{\text{O}}) H \phi_d(\mathbf{r}-\mathbf{r}_{\text{Cu}}) d\mathbf{r}, \quad (1)$$

where $H = -(\hbar^2/2m)\nabla^2 + U(\mathbf{r})$. $U(\mathbf{r})$ is the periodic potential in the crystal and may be expressed as $U(\mathbf{r}) = U_{\text{atom}}(\mathbf{r}) + U_{\text{M}}(\mathbf{r})$. $U_{\text{atom}}(\mathbf{r})$ is the contribution from atomic potentials, and $U_{\text{M}}(\mathbf{r})$ is the Madelung potential defined by $U_{\text{M}}(\mathbf{r}) = \sum_i V_i(\mathbf{r}-\mathbf{r}_i) = \sum_i Z_i e^2 / \epsilon_\infty |\mathbf{r}-\mathbf{r}_i|$ (Z_i is the valence of an ion at site i and ϵ_∞ the dielectric constant due to core polarization). Using these expressions, we obtain

$$t_{pd} = t_{pd}^0 + t_{pd}^{\text{M}}, \quad (2)$$

$$t_{pd}^0 = \int \phi_p^* \left(-\frac{\hbar^2}{2m} \nabla^2 + U_{\text{atom}} \right) \phi_d d\mathbf{r}, \quad (3)$$

$$t_{pd}^{\text{M}} = \int \phi_p^* V_{\text{M}} \phi_d d\mathbf{r}, \quad (4)$$

where $V_{\text{M}} \equiv \sum_i' V_i$ with the summation excluding two sites, on which the two orbitals, ϕ_p and ϕ_d , are sitting.¹⁷ For the right-hand side of Eq. (3), we use the two-center approximation as usual.¹⁸ Therefore, t_{pd}^0 term depends only on the distance $d_{\text{Cu-O}} \equiv |\mathbf{r}_{\text{Cu}} - \mathbf{r}_{\text{O}}|$. On the contrary, t_{pd}^{M} is dependent not only on $d_{\text{Cu-O}}$ but also on the crystal structure via V_{M} . t_{pp} is obtained by replacing ϕ_d in Eqs. (1), (3), and (4) with ϕ_p . In the evaluation of V_{M} , three sites, on which two ϕ_p 's and their neighboring ϕ_d are sitting, are excluded in the summation.¹⁷

We take the phase of the orbitals so as to make both t_{pd}^0 and t_{pp}^0 negative. Thus the smaller $t_{pd(pp)}^{\text{M}}$ is, the larger the absolute values of $t_{pd(pp)}$ is [see Eq. (2)]. We evaluate $t_{pd(pp)}^{\text{M}}$ numerically. The Wannier orbitals, ϕ_d and ϕ_p , can be constructed by atomic wave functions.¹⁹ We use the hydrogen-like atomic orbitals for the atomic wave functions. $t_{pd(pp)}^{\text{M}}$ is evaluated up to the order of $O(\mathcal{S}^1)$, where \mathcal{S} is the overlap integral between $\text{O}2p_x$ and its neighboring $\text{Cu}3d_{x^2-y^2}$ or $\text{O}2p_y$ atomic orbitals. The value of \mathcal{S} between $\text{Cu}3d_{x^2-y^2}$ and $\text{O}2p_x$ is assumed to be 0.03 at $d_{\text{Cu-O}} = 1.91 \text{ \AA}$ referring to those for other transition-metal oxides.²⁰ The special extent of the $\text{O}2p$ orbital is approximately fitted to the Hartree-Fock wave function for O^{2-} .²¹ The value of \mathcal{S} between $\text{O}2p_x$ and $\text{O}2p_y$ is then estimated to be 0.24 at $d_{\text{O-O}} = 2.69 \text{ \AA}$.

The calculated values of t_{pd}^{M} and t_{pp}^{M} for various materials are shown in Fig. 2. These values depend not only on material but also on the dimensionality of Cu-O network. These variations are caused by the difference of the spatial distri-

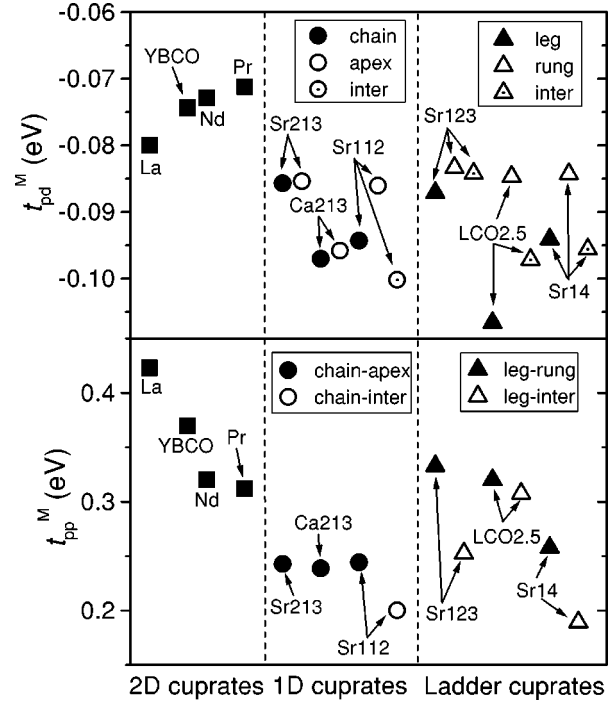


FIG. 2. The values of t_{pd}^{M} and t_{pp}^{M} calculated for the various cuprates. Each symbol in the 1D and ladder cuprates represents t_{pd}^{M} and t_{pp}^{M} for the bond related to each oxygen shown in Fig. 1. The labels attached to the data represent the compounds: ‘‘La’’ for La_2CuO_4 , ‘‘YBCO’’ for $\text{YBa}_2\text{Cu}_3\text{O}_{6+x}$, ‘‘Pr’’ for Pr_2CuO_4 , ‘‘Nd’’ for Nd_2CuO_4 , ‘‘Sr213’’ for Sr_2CuO_3 , ‘‘Ca213’’ for Ca_2CuO_3 , ‘‘Sr112’’ for SrCuO_2 , ‘‘Sr123’’ for SrCu_2O_3 , ‘‘LCO2.5’’ for $\text{LaCuO}_{2.5}$, and ‘‘Sr14’’ for $\text{Sr}_{14}\text{Cu}_{24}\text{O}_{41}$. The smaller $t_{pd(pp)}^{\text{M}}$ is, the larger the absolute values of $t_{pd(pp)}$ is.

bution of the Madelung potentials V_{M} around Cu and O, which is mainly determined by the local environment: (i) the number of negative O ions coordinated around Cu ions and (ii) the valence and number of positive ions such as Sr^{2+} , Y^{3+} and other Cu^{2+} located around Cu and O ions.

The values of t_{pd}^{M} and t_{pp}^{M} in 1D cuprates (middle panel) are smaller than those in 2D ones (left panel). This behavior mainly comes from the difference of the stacking patterns of the Cu-O network: in 2D the CuO_2 planes stack along the c axis with block layers inserted between the planes, whereas in 1D the Cu-O chains stack along the b axis without any layers between the chains. Such structural difference gives rise to the variation of the spatial distribution of the Madelung potentials around the Cu-O and O-O bonds. In particular, the magnitude of the Madelung potential around Cu and O ions in the 1D cuprates is enhanced by the presence of the Cu^{2+} ions in the adjacent Cu-O chains. This leads to the small values of t_{pd}^{M} and t_{pp}^{M} for the 1D cuprates. In the 2D cuprates, t_{pp}^{M} has a large difference among the materials. t_{pp}^{M} for La_2CuO_4 is larger than those for Nd_2CuO_4 and Pr_2CuO_4 . This is caused by the difference of the coordination number: six O ions in La_2CuO_4 , whereas four O ions in Nd_2CuO_4 . t_{pp}^{M} for $\text{YBa}_2\text{Cu}_3\text{O}_{6+x}$ with pyramidal coordination is located between La_2CuO_4 and Nd_2CuO_4 (Pr_2CuO_4).

From the above arguments, we can say that, when positive charges are close to Cu and O ions, $t_{pd(pp)}^{\text{M}}$ becomes small, and as a consequence $t_{pd(pp)}$ is enhanced. This mecha-

TABLE I. The parameters used in the cluster calculation for the typical cuprates. Listed are the hopping matrix elements between Cu3d and O2p orbitals, t_{pd} , and between neighboring O2p orbitals, t_{pp} , and the energy-level separation between Cu3d and O2p orbitals, Δ .

| | Material | $-t_{pd}$ (eV) | $-t_{pp}$ (eV) | Δ (eV) |
|-----------------|-------------------------------------|---|-------------------------|--------------------------------------|
| 2D cuprates | La ₂ CuO ₄ | 1.24 | 0.38 | 3.3 |
| | YBa ₂ CuO _{6+x} | 1.13 | 0.40 | 2.8 |
| | Nd ₂ CuO ₄ | 1.05 | 0.39 | 2.4 |
| 1D cuprates | Sr ₂ CuO ₃ | 1.16, ^a 1.09 ^b | 0.49 | 3.1, ^a 2.5 ^b |
| | Ca ₂ CuO ₃ | 1.24, ^a 1.10 ^b | 0.41 | 3.5, ^a 2.7 ^b |
| | SrCuO ₂ | 1.15, ^a 1.22, ^b 1.25 ^c | 0.53, 0.63 ^c | 3.5, ^a 3.0 ^b |
| Ladder cuprates | SrCu ₂ O ₃ | 1.08, ^d 1.15, ^e 1.29 ^f | 0.42, 0.53 ^f | 2.6, ^d 2.6 ^e |
| | LaCuO _{2.5} | 1.15, ^d 1.07, ^e 1.40 ^f | 0.33, 0.46 ^f | 2.77, ^d 2.86 ^e |

^aParallel to the chain.

^bPerpendicular to the chain.

^cInterchain direction.

^dLeg direction.

^eRung direction.

^fInterladder direction.

nism also makes a difference in two hopping matrix elements between O2p orbitals in the ladder cuprates. From Fig. 1, we find two types of O-O bond: (i) two Cu ions are located on both sides of the bond (bold lines in Fig. 1), and (ii) there is only one Cu ion on one side of the bond. The former is seen in the double chain compound SrCuO₂ and in the coupled ladder ones SrCu₂O₃ and Sr₁₄Cu₂₄O₄₁. The former bond shows the smaller t_{pp}^M as compared with the latter one. (See open circle and triangles in the lower panel in Fig. 2.) The resulting $|t_{pp}|$ in the former bond becomes larger (see Table I). This difference gives the anisotropic J in the coupled ladder compounds as will be discussed below.

In the following, we evaluate the value of J by using a Cu₂O₇ cluster with two holes.¹ The value of J is determined by the difference of the energy between the ground state with the total spin of $S_{\text{tot}}=0$ and the excited state with $S_{\text{tot}}=1$. The exact diagonalization method is used for the calculation of the energies. The parameters are obtained in the same way as the previous studies.²²⁻²⁴ The Hamiltonian is given by Eq. (1) of Ref. 23. The parameter Δ is determined by the difference in the Madelung potential between Cu and O, and the dielectric constant.¹⁶ By using the obtained Δ , the calculated gaps are in good agreement with the experimental values. For t_{pd}^0 and t_{pp}^0 , we take the bond length dependences with d^{-4} and d^{-3} , respectively. The values of t_{pd}^0 and t_{pp}^0 for La₂CuO₄ are assumed to be 1.15 eV and 0.80 eV, respectively. The resulting parameter values for typical cuprates are listed in Table I. The on-site Coulomb energies are set to be $U_d=8.5$ eV and $U_p=4.1$ eV. The Hund's coupling on O ion is assumed to be $K_p=0.6$ eV, and the direct exchange interaction between Cu3d and O2p is taken to be $K_{pd}=0.05$ eV as for the previous study.²³

The calculated J 's are presented in Fig. 3. The results show the characteristics seen in the experiments: (i) the values of J in the 1D cuprates are larger than those in 2D ones, and (ii) $J_{\text{leg}} > J_{\text{rung}}$ in the ladder cuprates. The variations of t_{pd}^M and t_{pp}^M on the dimensionality are their origin. In particu-

lar, the significant enhancements of t_{pd} and t_{pp} are crucial for obtaining large values of J in the 1D cuprates. If there were no such enhancements, J would be smaller than that in the 2D cuprates because of large values of Δ . The enhancement of t_{pp} between O(leg) and O(inter) in SrCu₂O₃ and Sr₁₄Cu₂₄O₄₁ is also important for the relation of $J_{\text{leg}} > J_{\text{rung}}$. The large t_{pp} induces the increase in J_{leg} , resulting in $J_{\text{leg}} > J_{\text{rung}}$ overcoming the effect of t_{pd} on J that makes J_{rung} larger than J_{leg} via a bond length relation, $d_{\text{leg}} > d_{\text{rung}}$.^{12,13} In contrast, the relation of $J_{\text{leg}} > J_{\text{rung}}$ in LaCuO_{2.5} comes from the fact that $d_{\text{leg}} < d_{\text{rung}}$.¹¹ Recently, the band structure calculations have been done for ladder cuprates Sr₁₄Cu₂₄O₄₁ and SrCu₂O₃.^{25,26} The tight binding fitting to the band structures shows that the effective hopping between nearest neighbor Cu sites along the legs of the ladder is larger by

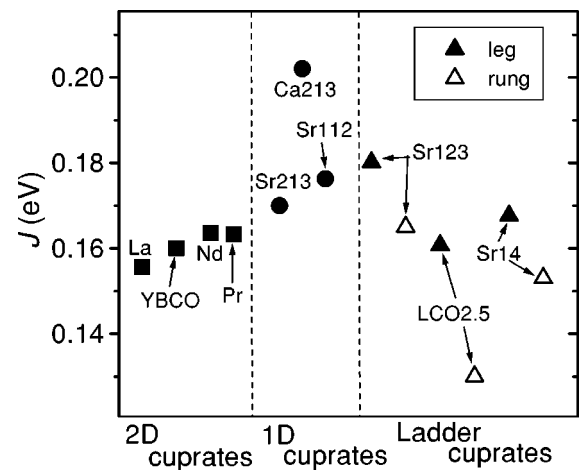


FIG. 3. The calculated value of the superexchange interaction J . The parameter values used in the calculation are listed in Table I. The labels represent the compounds; see the caption of Fig. 2. In the ladder cuprates, solid and open triangles represent J_{leg} and J_{rung} , respectively. The data qualitatively reproduce the tendencies seen in the experiments.

about 35% than that along the rungs. We believe that part of this difference comes from the enhancement of t_{pp} between O(leg) and O(inter), because the enhanced t_{pp} contributes only to the effective hopping along the legs as is easily understood from Fig. 1.

The calculated results of J in Fig. 3 reproduce the tendencies seen in the experiments very well. A detailed quantitative comparison is, however, difficult at present, because (i) in our evaluation of t_{pd} and t_{pp} , we neglect some possible effects such as the dependence of the spatial extent of atomic orbitals on the electron density, (ii) the experimental data of J are strongly dependent on the experimental tools, for instance, 0.18~0.26 eV for Sr_2CuO_3 (Refs. 4–6) and 0.13~0.16 eV,^{1–3} (iii) the next-nearest-neighbor exchange interaction J' (Ref. 27) and the four-spin interaction J_4 (Ref. 28) which are involved in 2D and ladder cuprates prevent the direct comparison between the experimental and theoretical J 's.²⁹ It is, therefore, necessary to make efforts from both

experimental and theoretical sides to draw a quantitative comparison.

In summary, we have investigated the superexchange interaction in the various types of cuprates. The interaction strongly depends on the local environments through the modification of hopping matrix elements due to the Madelung potentials. The enhanced J in the 1D cuprates and the anisotropy of J_{leg} and J_{rung} in the ladder compounds show a unique dependence of the electronic structure on dimensionality.

This work was supported by a Grant-in-Aid for Scientific Research on Priority Areas from the Ministry of Education, Science, Sports and Culture of Japan. Parts of the numerical calculation were performed in the Supercomputer Center, Institute for Solid State Physics, University of Tokyo, and the supercomputing facilities in Institute for Materials Research, Tohoku University. Y.M. would like to thank the Japan Society for the promotion of science for financial support.

*On leave from Department of Applied Physics, Nagoya University, Nagoya 464-8601, Japan.

¹Y. Ohta, T. Tohyama, and S. Maekawa, Phys. Rev. Lett. **66**, 1228 (1991) and references therein.

²P. Bourges, H. Casalta, A. S. Ivanov, and D. Petitgrand, Phys. Rev. Lett. **79**, 4906 (1997).

³S. M. Hayden, G. Aeppli, P. Dai, H. A. Mook, T. G. Perring, S.-W. Cheong, Z. Fisk, F. Doğan, and T. E. Mason, Physica B **241-243**, 765 (1998).

⁴T. Ami, M. K. Crawford, R. L. Harlow, Z. R. Wang, D. C. Johnston, Q. Huang, and R. W. Erwin, Phys. Rev. B **51**, 5994 (1995).

⁵N. Motoyama, H. Eisaki, and S. Uchida, Phys. Rev. Lett. **76**, 3212 (1996).

⁶H. Suzuura, H. Yasuhara, A. Furusaki, N. Nagaosa, and Y. Tokura, Phys. Rev. Lett. **76**, 2579 (1996).

⁷D. C. Johnston, Phys. Rev. B **54**, 13 009 (1996).

⁸R. S. Eccleston, M. Uehara, J. Akimitsu, H. Eisaki, N. Motoyama, and S. Uchida, Phys. Rev. Lett. **81**, 1702 (1998).

⁹T. Imai, K. R. Thumber, K. M. Shen, A. W. Hunt, and F. C. Chou, Phys. Rev. Lett. **81**, 220 (1998).

¹⁰Chr. L. Teske and Hk. Müller-Buschbaum, Z. Anorg. Allg. Chem. **371**, 325 (1969); *ibid.* **379**, 234 (1970).

¹¹Z. Hiroi and M. Takano, Nature (London) **377**, 41 (1995).

¹²M. Azuma, Z. Hiroi, M. Takano, K. Ishida, and Y. Kitaoka, Phys. Rev. Lett. **73**, 3463 (1994).

¹³E. M. McCarron III, M. A. Subramanian, J. C. Calabrese, and R. L. Harlow, Mater. Res. Bull. **23**, 1355 (1988).

¹⁴H. Eskes and J. H. Jefferson, Phys. Rev. B **48**, 9788 (1993).

¹⁵M. Imada, A. Fujimori, and Y. Tokura, Rev. Mod. Phys. **70**, 1039 (1998).

¹⁶The experimental indication of large Δ in the 1D cuprates is con-

sistent with our theoretical estimate. Δ may be written as $\Delta = \Delta V_M/\epsilon_\infty + \Delta_0$, where ΔV_M is the difference in the Madelung site potentials for a hole between Cu and O, ϵ_∞ is the dielectric constant, and Δ_0 involves the second ionization energy of the Cu^{2+} ion and the second electron affinity of the O^{2-} ion. We set ϵ_∞ to be 3.5 for the 2D and ladder compounds (Refs. 22 and 23) and 3.3 for 1D (Ref. 23), taking into account the number of oxygen in the Cu-O network. The small ϵ_∞ in 1D cuprates causes large Δ .

¹⁷The exclusion of those sites in the summation is done to avoid the divergence of the Coulomb potential due to point charge in the integration in Eq. (4). The excluded terms are almost independent of material.

¹⁸J. C. Slater and G. Koster, Phys. Rev. **94**, 1498 (1954).

¹⁹P.-O. Löwdin, J. Chem. Phys. **18**, 365 (1950).

²⁰L. F. Mattheiss, Phys. Rev. B **5**, 290 (1972).

²¹R. E. Watson, Phys. Rev. **111**, 1108 (1958).

²²Y. Ohta, T. Tohyama, and S. Maekawa, Phys. Rev. B **43**, 2968 (1991).

²³Y. Mizuno, T. Tohyama, S. Maekawa, T. Osafune, N. Motoyama, H. Eisaki, and S. Uchida, Phys. Rev. B **57**, 5326 (1998).

²⁴Y. Mizuno, T. Tohyama, and S. Maekawa, J. Phys. Soc. Jpn. **66**, 937 (1997).

²⁵M. Arai and H. Tsunetsugu, Phys. Rev. B **56**, R4305 (1997).

²⁶T. F. A. Müller, V. Anisimov, T. M. Rice, I. Dasgupta, and T. Saha-Dasgupta, Phys. Rev. B **57**, R12 655 (1998).

²⁷D. K. Morr, Phys. Rev. B **58**, R587 (1998).

²⁸H. J. Schmidt and Y. Kuramoto, Physica C **167**, 263 (1990).

²⁹We note that J' and J_4 enlarge the difference of the observed J 's between the 1D and 2D cuprates (Refs. 27 and 28), and the anisotropy in the ladder cuprates [N. Nagaosa (private communication)].